AMERICAN SOCIETY FOR MICROBIOLOGY | Applied and Environmental Microbiology®

GENETICS AND MOLECULAR BIOLOGY

Monothiol Glutaredoxin Is Essential for Oxidative Stress Protection and Virulence in *Pseudomonas aeruginosa*

Kritsakorn Saninjuk,[a] Adisak Romsang,[b,c] Jintana Duang-nkern,[a] Lampet Wongsaroj,[a] Panithi Leesukon,[d] James M. Dubbs,[a] Paiboon Vattanaviboon,[a,e,f] Skorn Mongkolsuk[a]

[a]Laboratory of Biotechnology, Chulabhorn Research Institute, Bangkok, Thailand
[b]Department of Biotechnology, Faculty of Science, Mahidol University, Bangkok, Thailand
[c]Center for Emerging Bacterial Infections, Faculty of Science, Mahidol University, Bangkok, Thailand
[d]Molecular Medicine Graduate Program, Faculty of Science, Mahidol University, Bangkok, Thailand
[e]Center of Excellence on Environmental Health and Toxicology (EHT), the Office of the Permanent Secretary, Ministry of Higher Education, Science, Research and Innovation, Bangkok, Thailand
[f]Program in Applied Biological Sciences: Environmental Health, Chulabhorn Graduate Institute, Chulabhorn Royal Academy, Bangkok, Thailand

ABSTRACT Glutaredoxins (Grxs), ubiquitous redox enzymes belonging to the thioredoxin family, catalyze the reduction of thiol-disulfide exchange reactions in a glutathione-dependent manner. A *Pseudomonas aeruginosa* Δ*grxD* mutant exhibited hypersensitivity to oxidative stress-generating agents, such as paraquat (PQ) and cumene hydroperoxide (CHP). *In vitro* studies showed that *P. aeruginosa* GrxD acts as an electron donor for organic hydroperoxide resistance enzyme (Ohr) during CHP degradation. The ectopic expression of iron-sulfur cluster ([Fe-S]) carrier proteins, including ErpA, IscA, and NfuA, complements the function of GrxD in the Δ*grxD* mutant under PQ toxicity. Constitutively high expression of *iscR*, *nfuA*, *tpx*, and *fprB* was observed in the Δ*grxD* mutant. These results suggest that GrxD functions as a [Fe-S] cluster carrier protein involved in [Fe-S] cluster maturation. Moreover, the Δ*grxD* mutant demonstrates attenuated virulence in a *Drosophila melanogaster* host model. Altogether, the data shed light on the physiological role of GrxD in oxidative stress protection and virulence of the human pathogen, *P. aeruginosa*.

IMPORTANCE Glutaredoxins (Grxs) are ubiquitous disulfide reductase enzymes. Monothiol Grxs, containing a CXXS motif, play an essential role in iron homeostasis and maturation of [Fe-S] cluster proteins in various organisms. We now establish that the human pathogen *Pseudomonas aeruginosa* GrxD is crucial for bacterial virulence, maturation of [Fe-S] clusters and facilitation of Ohr enzyme activity. GrxD contains a conserved signature monothiol motif (C_{29}GFS), in which C29 is essential for its function in an oxidative stress protection. Our findings reveal the physiological roles of GrxD in oxidative stress protection and virulence of *P. aeruginosa*.

KEYWORDS monothiol glutaredoxin, oxidative stress, virulence, *Pseudomonas aeruginosa*

Pseudomonas aeruginosa is an opportunistic human pathogen that can infect a wide range of hosts, including plants, invertebrates, and vertebrates. *P. aeruginosa* causes health care-associated infections in immunocompromised patients, such as urinary tract infections, dermatitis, soft tissue infections, bacteremia, bone and joint infections, surgical wound infections, and pneumonia (1). Moreover, individuals with debilitating disorders such as cystic fibrosis are prone to infections with *P. aeruginosa*, which is also the leading cause of sight-threatening microbial keratitis in healthy individuals using contact lenses (2, 3). During the infection process, this bacterium is exposed to reactive oxygen species (ROS) generated by host phagocytic cells as part of the innate immune defense system (4). The ROS, i.e., superoxide anion ($O_2^{\cdot -}$), hydrogen peroxide (H_2O_2), and hydroxyl radical ($^{\cdot}OH$), cause

Editor Ning-Yi Zhou, Shanghai Jiao Tong University

Address correspondence to Skorn Mongkolsuk, skorn@cri.or.th.

The authors declare no conflict of interest.

Received 5 October 2022
Accepted 24 November 2022

oxidative damage to biological macromolecules, including nucleic acids, lipids, and proteins, especially the [Fe-S] cluster-containing proteins (5). The ability to eliminate oxidative stress is a key strategy that allows bacteria to survive in the host and cause diseases. *P. aeruginosa* produces both enzymatic and nonenzymatic antioxidants to defend against oxidative stress. For instance, it upregulates antioxidant enzymes, superoxide dismutases (Sods), catalases, and alkyl hydroperoxide reductases to detoxify $O_2^{\cdot-}$, H_2O_2, and organic peroxides, respectively (6, 7). *P. aeruginosa* also produces glutathione and thioredoxin as nonenzymatic antioxidants to protect itself from these stressors (8, 9).

Glutaredoxins (Grxs) are small disulfide reductase enzymes of approximately 100 amino acids that use reduced glutathione (GSH) and NADPH as cofactors (10). Grxs are divided into class I, dithiol Grxs (CXXC), and class II, monothiol Grxs (CXXS) according to the number of cysteine residues (C) in the active site motif (10–13). In yeasts, monothiol Grxs play essential roles in intracellular iron signaling, iron trafficking, and maturation of [Fe-S] cluster proteins (10). The lack of the Grx5 in *Saccharomyces cerevisiae* greatly increases sensitivity to oxidative damage mediated by the redox-cycling drug menadione and H_2O_2 (14). This is consistent with the finding that an absence of *grx5* decreases activity of [Fe-S] cluster-containing enzymes, such as aconitase and succinate dehydrogenase, resulting in iron accumulation that promotes intracellular oxidative damage (15).

Escherichia coli contains a single domain CGFS-type monothiol Grx, Grx4, that is encoded by *grxD*. Grx4 is directly involved in iron regulation via interaction with the global iron-uptake regulator, Fur. In *E. coli*, the expression level of *grxD* significantly increases in a *fur* mutant, suggesting that Fur either directly or indirectly regulates *grxD* expression (16). A *grxD* mutant shows synthetic lethality when simultaneous mutations occur in key component genes in the iron-sulfur cluster biogenesis (*isc*) operon, suggesting a contribution of Grx4 to [2Fe-2S] cluster biogenesis. In addition, *E. coli* Grx4 can form [2Fe-2S] cluster-bound homodimeric and heterodimeric complexes with BolA-like protein that can function as scaffold proteins for [2Fe-2S] clusters (11, 17). BolA-like proteins exist in both prokaryotes and eukaryotes, where they are thought to control the expression levels of transcriptional regulators involved in maintaining cell morphology and cell division (10, 18). Moreover, Grx4 and NfuA are known to be crucial for activity of an [Fe-S] cluster-containing tRNA modification enzyme (19).

Iron-sulfur clusters are essential cofactors present in numerous enzymes and proteins that are involved in a variety of cellular functions, such as electron transfer, enzymatic catalysis, gene regulation, and central metabolism (20, 21). However, [Fe-S] clusters are readily damaged by univalent oxidants, leading to protein inactivation and a release of ferrous ions (Fe^{2+}) that subsequently undergo the Fenton reaction to produce highly toxic hydroxyl radicals. Damaged [Fe-S] clusters are rebuilt by the adaptive expression of the [Fe-S] cluster biogenesis genes, such as those of the iron-sulfur cluster (ISC), sulfur utilization (SUF), and nitrogen fixation (Nif) systems. The damaged cluster can also be repaired by ferredoxin NADP(+) reductase (Fpr). Fpr is a flavin adenine dinucleotide (FAD)-containing oxidoreductase enzyme that mediates a reversible redox reaction between NADPH and electron carrier [Fe-S] clusterproteins (22). Sulfur is provided by cysteine via cysteine desulfurases (IscS, SufS, and NifS). Scaffold proteins, such as IscU, IscA, SufU, SufA, and NifU, form an intermediate assembly site for [Fe-S] cluster precursors before cluster transfer to the target apo-proteins (23).

In *P. aeruginosa*, the physiological function of GrxD is yet unclear. Inactivation of *grxD* renders *P. aeruginosa* more susceptible to polymyxin antibiotics than its parental strain (24). In this study, the physiological functions of *P. aeruginosa* GrxD under oxidative stress were investigated. In addition, GrxD's role in the pathogenicity of *P. aeruginosa* was evaluated.

RESULTS

***grxD* mutant has defects in growth and colony formation.** The *P. aeruginosa* PAO1 genome (25) contains a 108-amino acid protein annotated as monothiol

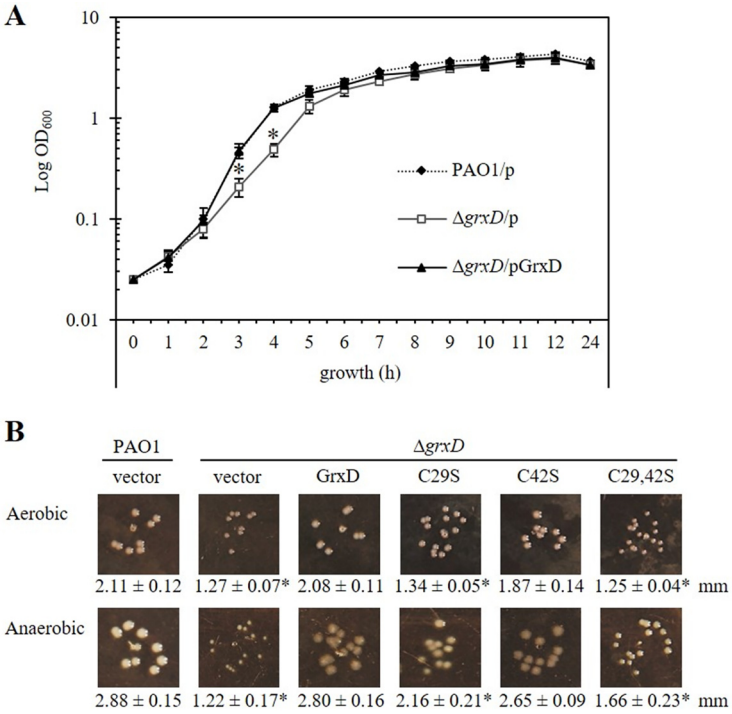

FIG 1 Aerobic and anaerobic growth curves and colony morphology of *P. aeruginosa* strains. (A) Growth of *P. aeruginosa* strains under aerobic conditions was determined in LB broth medium incubated at 37°C with shaking at 180 rpm. Asterisks indicate statistical significance ($P < 0.05$) determined by one-way analysis of variance (ANOVA) and Tukey's test relative to PAO1/p. (B) The colony morphology of PAO1 and Δ*grxD* mutant strains was determined under aerobic and anaerobic growth conditions. The numbers beneath the colony figures represent the means ± standard deviation (SD) of colony size of *P. aeruginosa* strains ($n = 10$). The asterisks indicate statistical significance (paired *t* test, $P < 0.05$) compared with PAO1 treated under the same condition. Bacteria were grown in LB agar for aerobic conditions and in LB agar plus 1% KNO_3 for anaerobic conditions.

glutaredoxin (*grxD*). Deletion of *grxD* enhances susceptibility to polymyxin antibiotics relative to parental PAO1 (24). The polymyxin susceptibility of the mutant was observed during both aerobic and anaerobic growth, suggesting that the *grxD* mutant (Δ*grxD*) phenotype does not involve hydroxyl radicals generated from antibiotic treatment (24). Here, the growth curve of the Δ*grxD* mutant grown under aerobic conditions in LB medium was determined and compared with that of PAO1. The Δ*grxD* mutant grew more slowly during log phase compared to PAO1 (Fig. 1A). The log-phase growth phenotype of the Δ*grxD* mutant was restored to that of PAO1 in the complemented mutant (Δ*grxD*/pGrxD) (Fig. 1A). We next observed the colony morphology and measured the colony diameter of the Δ*grxD* mutant and PAO1. The results in Fig. 1B showed that the Δ*grxD* mutant colonies were significantly reduced in size compared to those of PAO1 in both aerobic (PAO1/p, 2.11 ± 0.12 mm; Δ*grxD*/p, 1.27 ± 0.07 mm; and Δ*grxD*/pGrxD, 2.08 ± 0.11 mm) and anaerobic (PAO1/p, 2.88 ± 0.15 mm; Δ*grxD*/p, 1.22 ± 0.17 mm; and Δ*grxD*/pGrxD, 2.80 ± 0.16 mm) conditions (Fig. 1B). However, the number of colonies was not significantly different under the two conditions.

To test whether reduced colony size of the Δ*grxD* strain was related to bacterial cell size, the length of bacterial cells from the exponential-phase cultures (after 3 h of growth) was measured, and the results are shown in Fig. 2A and B. The length of PAO1 carrying pBBR1MCS-4 vector (PAO1/p) was 2.45 ± 0.12 μm. The length of the Δ*grxD* mutant (Δ*grxD*/p, 2.20 ± 0.12 μm) cells was significantly shorter than PAO1/p (Fig. 2B), and this altered phenotype could be restored in the complemented mutant strain (Δ*grxD*/pGrxD, 2.53± 0.17 μm). Therefore, the reduced bacterial cell size of the Δ*grxD* mutant, at least in part, accounted for the reduced colony size of the mutant.

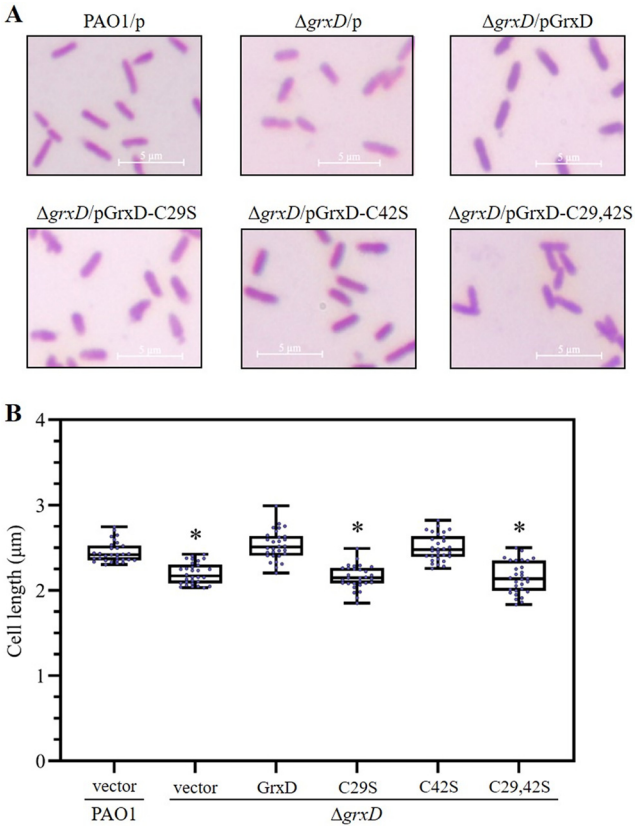

FIG 2 Determination of cell length in *P. aeruginosa* strains. (A) Exponential cells of *P. aeruginosa* strains (PAO1/p, Δ*grxD*/p, Δ*grxD*/pGrxD, Δ*grxD*/pGrxD-C29S, Δ*grxD*/pGrxD-C42S, and Δ*grxD*/pGrxD-C29S,C42S) were Gram stained, and the images were photographed through a light microscope. (B) The cell lengths were measured using the same scale bar adjustment. The data shown are the means ± SD from five independent cultures ($n = 30$). Asterisks indicate significant differences compared to PAO1/p according to Dunnett's *post hoc* test ($P < 0.05$).

Physiological role of GrxD in an oxidative stress response. The physiological roles of *grxD* in stress responses were assessed. Plate sensitivity assay was used to determine the resistance levels against a redox-cycling drug (paraquat [PQ]), an iron-depleting agent (2,2′-dipyridyl [Dipy]), a thiol-depleting agent (*N*-ethylmaleimide [NEM]), hydrogen peroxide (H_2O_2), and organic hydroperoxides (*tert*-butyl hydroperoxide [tBH] and cumene hydroperoxide [CHP]) in the Δ*grxD* mutant, complemented mutant (Δ*grxD*/pGrxD), and PAO1 strains. The results in Fig. 3A showed that the Δ*grxD* mutant (Δ*grxD*/p) was 10^3-, 30-, 100-, and 60-fold more sensitive to PQ, Dipy, tBH, and CHP, respectively, than its parental PAO1. Exposure of the strains Δ*grxD*, Δ*grxD*/pGrxD, and PAO1 to heat stress (50°C for 15 and 30 min) showed no significant differences in the percentage of survival, indicating that *P. aeruginosa* GrxD is not required for survival under heat stress (Fig. 3A). Thus, these results indicated that *grxD* plays a crucial role in protecting PAO1 from oxidative stress generated from paraquat and organic hydroperoxides.

Functional analysis of conserved cysteine residues of GrxD. *P. aeruginosa* GrxD contains two cysteine residues, C29 and C42. C29 is a highly conserved cysteine residue that is located in the CGFS motif of the monothiol Grx domain, while C42 is a non-conserved cysteine residue found in certain GrxDs. The roles of these cysteine residues in GrxD functions were investigated. The Δ*grxD* mutant strains expressing mutated C29S, C42S, and C29S,C42S GrxD from pGrxD-C29S, pGrxD-C42S, and pGrxD-C29S,C42S plasmids (24) were tested for their ability to complement various Δ*grxD* mutant phenotypes. First, the reduced colony size of the Δ*grxD* mutant harboring various mutated GrxD constructs was determined under aerobic and anaerobic conditions. In Fig. 1B,

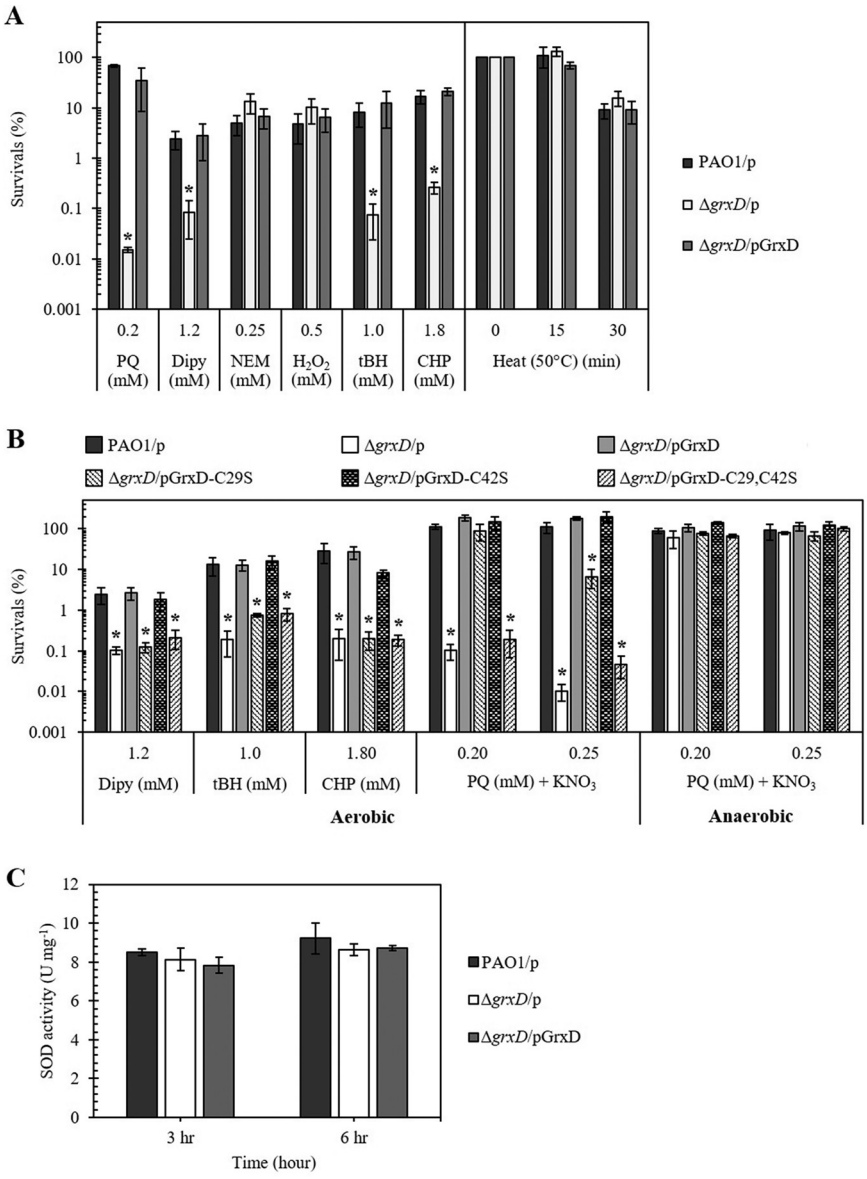

FIG 3 Determination of oxidant resistance levels in *P. aeruginosa* strains. (A) The resistance levels of PAO1and Δ*grxD* mutant strains harboring empty vector (PAO1/p and Δ*grxD*/p), and the complemented mutants (Δ*grxD*/pGrxD) against various oxidants were determined using plate sensitivity assay on plates containing the oxidants 0.2 mM paraquat (PQ), 1.2 mM 2,2′-dipyridyl (Dipy), 0.25 mM *N*-ethylmaleimide (NEM), 0.5 mM H_2O_2, 1.0 mM *tert*-butyl hydroperoxide (tBH), and 1.8 mM cumene hydroperoxide (CHP). (B) Plate sensitivity assays of PAO1/p, Δ*grxD*/p, and Δ*grxD* mutant complemented with wild-type GrxD or C29S and/or C42S GrxD (Δ*grxD*/pGrxD, Δ*grxD*/pGrxD-C29S, Δ*grxD*/pGrxD-C42S, and Δ*grxD*/pGrxD-C29S,C42S) were performed using LB plates plus 1% KNO_3 and incubated under aerobic and anaerobic atmospheres against 1.2 mM Dipy, 1.0 mM tBH, 1.8 mM CHP, and 0.20 or 0.25 mM PQ. Survival (%) was defined as the percentage of CFU on oxidant-containing plates over the number of CFU on oxidant-free plates. (C) Total superoxide dismutase (SOD) activity was determined in *P. aeruginosa* strains (PAO1/p, Δ*grxD*/p, and Δ*grxD*/pGrxD) and measured in exponential (3 h) and stationary (6 h) phase. The data shown are the means ± SD from three independent experiments. Asterisks indicate statistical significance (paired *t* test, $P < 0.05$) compared with PAO1 treated under the same condition.

the colonies on LB agar plate of Δ*grxD*/pGrxD-C29S and Δ*grxD*/pGrxD-C29S,C42S mutants grown under aerobic and anaerobic conditions were significantly smaller than those of the PAO1 wild type. However, Δ*grxD*/pGrxD-C29S had slightly larger colonies than the vector control, Δ*grxD*/p, while Δ*grxD*/pGrxD-C29S,C42S produced small colonies similar in size to those of the Δ*grxD* mutant. The expression of *grxD*-C42S could fully complement the phenotype of the Δ*grxD* mutant under aerobic (1.87 ± 0.14 mm)

and anaerobic (2.65 ± 0.09 mm) conditions (Fig. 1B). The colony size was also directly related to the observed cell size (Fig. 2).

Complementation analysis of increased oxidative stress-sensitive phenotypes of the Δ*grxD* mutant was performed. The CHP, tBH, and Dipy plate sensitivity assays showed that expression of *grxD*-C29S could not complement the increased sensitivity phenotype of the Δ*grxD* mutant. In contrast, the mutated GrxD-C29S fully complemented the PQ-sensitive phenotype at 0.2 mM but partially complemented at 0.25 mM (30-fold less than wild-type GrxD) (Fig. 3B). The expression of *grxD*-C42S fully complemented the mutant CHP-, tBH-, Dipy-, and PQ-sensitive phenotypes to the wild-type levels (Fig. 3B). As expected the expression of the doubly mutated *grxD*-C29S,C42S could not complement the mutant oxidant-sensitive phenotypes (Fig. 3B). The data suggested that the C29 residue of the CGFS motif, but not the nonconserved C42, is essential for GrxD function in PAO1 against PQ, organic hydroperoxide, and iron starvation stresses.

PQ-sensitive phenotype of Δ*grxD* mutant arises from the O_2-mediated toxicity. PQ is a superoxide generator and a redox-cycling drug. PQ toxicity can arise from either generating superoxide anion in the presence of oxygen (O_2) by disrupting electron transport chain or by its involvement in redox-cycling reactions (26). In order to test whether the PQ-sensitive phenotype of the Δ*grxD* mutant arose from PQ-mediated generation of superoxide anion or redox-cycling reactions, PQ plate sensitivity assays were performed under aerobic and anaerobic conditions. LB medium was supplemented with potassium nitrate (KNO_3, 1% wt/vol) as an alternative electron acceptor for anaerobic growth (27). Under aerobic conditions, the Δ*grxD* mutant showed 10^3- and 10^4-fold increased sensitivity to 0.2 and 0.25 mM PQ, respectively, and the phenotype was fully complemented in strain Δ*grxD*/pGrxD (Fig. 3A and B).

The experiments were repeated under anaerobic culture conditions. The results showed the Δ*grxD* mutant, Δ*grxD*/pGrxD-C29S, Δ*grxD*/pGrxD-C42S, and Δ*grxD*/pGrxD-C29S,C42S strains did not display a PQ-sensitive phenotype (Fig. 3B). The growth of both the *grxD* mutant and complemented strains expressing variant GrxD proteins were similar to that of wild-type PAO1 under anaerobic conditions (Fig. 3B). Therefore, the PQ toxicity phenotype of the Δ*grxD* mutant could be due to PQ ability to generate superoxide anions in the presence of O_2.

A previous study in the fungus *Beauveria bassiana* revealed that a Δ*grx5* mutant showed increased sensitivity to the superoxide generator, menadione, due to reduced superoxide dismutase (Sod) activity (28). *P. aeruginosa* has two Sod isozymes, a manganese Sod (SodA) and an iron Sod (SodB), and inactivation of *sod* increases PQ sensitivity (29). To test whether the PQ-sensitive phenotype of the Δ*grxD* mutant was due to altered levels of Sod activity, total Sod activity assays were performed. The results showed no significant difference in the levels of Sod activity between the Δ*grxD* mutant and the wild-type PAO1 in both exponential and stationary-phase cells (Fig. 3C). Thus, the PQ-sensitive phenotype of the Δ*grxD* mutant was not due to lowered Sod activity levels.

***P. aeruginosa* monothiol glutaredoxin facilitates the degradation of cumene hydroperoxide via Ohr.** Phenotypic analysis clearly showed that the Δ*grxD* mutant was hypersensitive to organic hydroperoxides but not other peroxides (Fig. 3A). Hence, the ability to degrade CHP was further evaluated in the Δ*grxD* mutant and the Δ*grxD* mutant complemented with plasmid pGrxD (Δ*grxD*/pGrxD) using ferrous ion oxidation xylenol orange (FOX) assays. The Δ*grxD* mutant, Δ*grxD*/pGrxD, and PAO1 strains were incubated with CHP, and the rate of hydroperoxide degradation was determined. After 30 min incubation, the amount of CHP remaining was 45% for the Δ*grxD* mutant and 30% for both the PAO1 and Δ*grxD*/pGrxD (Fig. 4A). The results indicated that the Δ*grxD* mutant had a significant reduction in the ability to metabolize CHP, which was rescued by GrxD complementation (Fig. 4A). These observations indicate that GrxD plays a role in the enzymatic degradation of CHP.

The thiol peroxidase, Ohr, is the major bacterial organic hydroperoxide detoxification enzyme (30–32). In many bacteria, inactivation of *ohr* renders cells hypersensitive to organic hydroperoxides (31, 33). Hence, the physiological roles of GrxD and Ohr in the

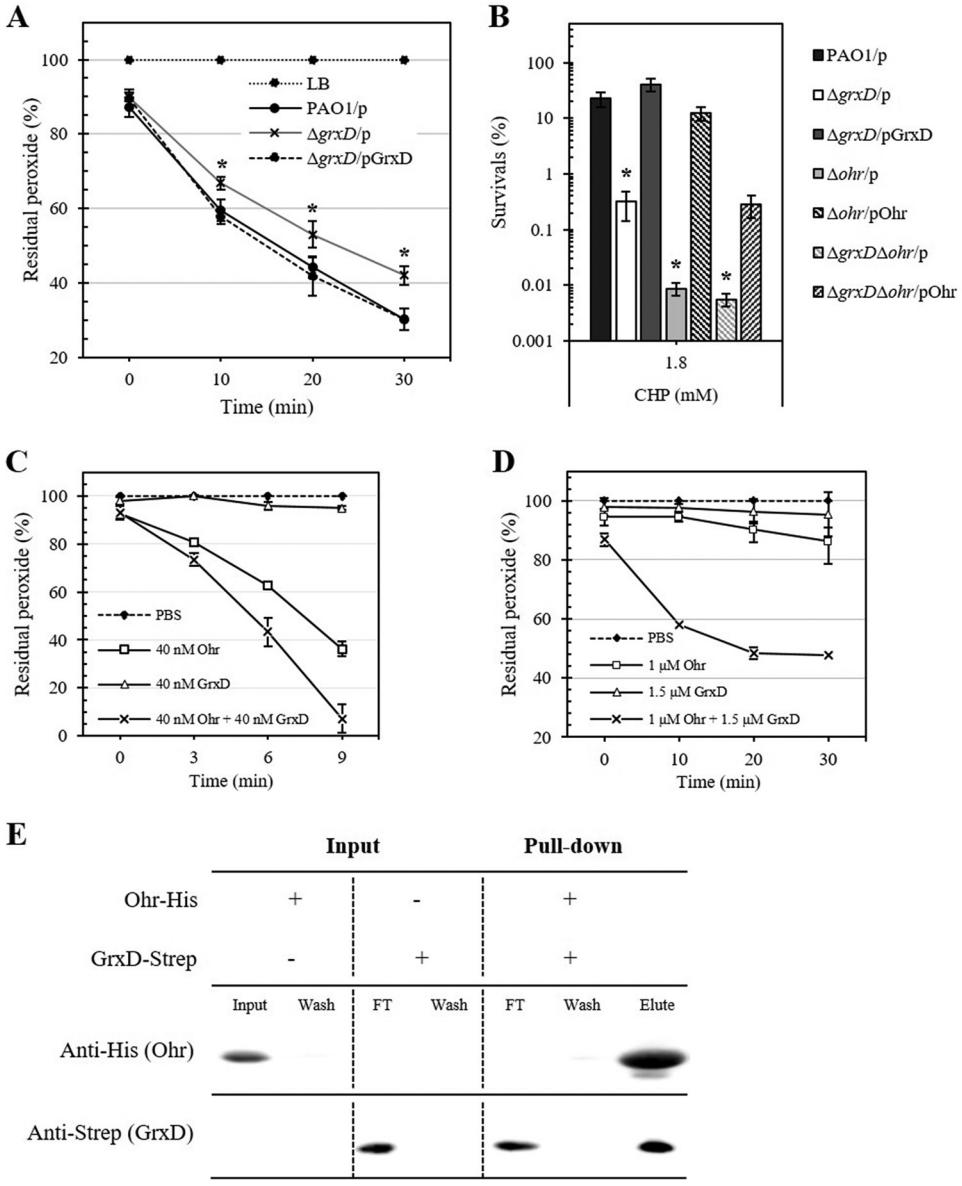

FIG 4 Determination of cumene hydroperoxide degradation and oxidant resistance levels of *P. aeruginosa* strains. (A) The rates of CHP degradation in culture medium containing 100 μM CHP by *P. aeruginosa* wild type (PAO1/p), *grxD* mutant (Δ*grxD*/p), and the complemented mutant (Δ*grxD*/pGrxD) were determined using FOX assay. LB represents a medium control without bacteria. (B) The oxidant resistance levels of *P. aeruginosa* PAO1, Δ*grxD*, and Δ*grxD*,Δ*ohr* mutants harboring either an empty vector (p), or an expression plasmid: pGrxD or pOhr. The resistance levels against 1.8 mM CHP were determined using a plate sensitivity assay. The data shown are the means ± SD of three independent experiments. Asterisks indicate statistically significant differences ($P < 0.05$) relative to PAO1/p. (C, D) The kinetics of CHP degradation in the presence of purified Ohr with (C) or without (D) 100 μM dithiothreitol (DTT) and in the presence or absence of purified GrxD. The data shown are the means ± SD of three independent experiments. (E) The interaction between Strep tag GrxD and His tag Ohr was determined using an *in vitro* pulldown assay. Complexes between GrxD and Ohr were immobilized with cobalt resin beads and detected by Western blotting analysis using anti-His tag and anti-Strep tag antibodies. (+) and (−) indicate the presence and absence of proteins. PBS, phosphate-buffered saline; FT, flow through.

protection of PAO1 from CHP were investigated by mutational analysis. A Δ*grxD*,Δ*ohr* double mutant was constructed to evaluate the possible interactions between GrxD and Ohr in CHP metabolism. We proposed that if GrxD contributes to Ohr function, the CHP sensitivity of the Δ*grxD*,Δ*ohr* double mutant should be the same as the Δ*ohr* mutant. Conversely, if GrxD plays no role in Ohr activity or if CHP sensitivity of the mutants arose from different pathways, then one would expect an increase in CHP sensitivity in the

double mutant compared to the single Δ*ohr* mutant. The results in Fig. 4B show that the Δ*grxD*,Δ*ohr* double mutant and the Δ*ohr* single mutant had similar levels of CHP sensitivity (10^3-fold more sensitive than PAO1). The CHP-sensitive phenotypes of Δ*grxD* and Δ*ohr* mutants were fully complemented by pGrxD and pOhr plasmids, respectively, while the CHP-sensitive phenotype of the double mutant was only partially complemented by pOhr (50-fold lower than PAO1) (Fig. 4B). Therefore, GrxD likely contributes to CHP resistance through Ohr.

In bacteria, Ohr enzymes are cysteine-based thiol peroxidases (32). The organic hydroperoxide decomposition of purified Ohr requires reducing agents such as dithiols (dithiothreitol [DTT] and dihydrolipoamide [DHLA]), but not monothiols (GSH and β-mercaptoethanol), for its activity (32, 34). Phenotypic evidence suggests that GrxD and Ohr might function together. The role of monothiol GrxD on Ohr activity *in vitro* was tested. The ability of purified Ohr to degrade CHP was evaluated using FOX assays in the presence and absence of purified GrxD. As shown in Fig. 4C, in the presence of dithiol DTT (100 μM), the ability to degrade CHP in the presence of 40 nM GrxD (95.0 $\pm$ 0.7% residual) was not different from that of the phosphate-buffered saline (PBS) control (100.0 $\pm$ 0.0% residual) after 9 min of incubation. Consistent with previous reports (34, 35), Ohr efficiently degraded CHP in the presence of DTT (36.2 $\pm$ 3.0% residual after 9 min incubation) (Fig. 4C). Interestingly, the reaction with DTT, 40 nM Ohr, and 40 nM GrxD was significantly more efficient than 40 nM Ohr alone after 9 min incubation (7.2 $\pm$ 5.8% compared with 36.2 $\pm$ 3.0% CHP residual) (Fig. 4C). The calculated K_m values for the assays either with or without GrxD clearly showed an increased K_m of the reaction in the presence of GrxD (40 nM Ohr, 27.53 $\pm$ 1.52 μM; and 40 nM Ohr + 40 nM GrxD, 23.50 $\pm$ 1.60 μM). These data indicate that the monothiol GrxD increased the peroxidase activity of Ohr in the presence of the dithiol DTT.

The results raise the question of whether GrxD alone could function as a sole reductant of the Ohr. The FOX assays were repeated without addition of DTT into the reaction. The ability to degrade CHP in the presence of GrxD but without DTT (95.4 $\pm$ 7.4% residual) was similar to that of the PBS control (100.0 $\pm$ 0.0% residual) after 30 min incubation (Fig. 4D). The reaction mixture containing 1.0 μM Ohr without DTT has 86.1 $\pm$ 4.8% residual CHP, while addition of 1.5 μM GrxD to a reaction mixture containing 1.0 μM Ohr showed only 46 $\pm$ 3.0% residual CHP after 30 min of incubation (Fig. 4D). The data suggest that without dithiol (DTT), GrxD can facilitate the peroxidase activity of Ohr *in vitro*. Therefore, there is a possibility that monothiol GrxD might be an alternative electron donor for Ohr in *P. aeruginosa*.

Next, an interaction between GrxD and Ohr was determined using *in vitro* pulldown assay. Purified Strep tag GrxD (400 μg) was incubated with 6$\times$ His tag Ohr (100 μg) bound to cobalt resin beads. The GrxD-Ohr complexes were detected by Western blot analysis using anti-His tag and anti-Strep tag antibodies. The results in Fig. 4E show an apparent binding between GrxD and Ohr proteins. These results confirmed that GrxD can directly interact with Ohr *in vitro*.

Deletion of *grxD* enhances expression of genes in the IscR regulon. Monothiol Grx has been proposed to be involved in [Fe-S] cluster delivery and maturation (10, 11, 17). Hence, we tested the activities of succinate dehydrogenase and aconitase, both of which are [4Fe-4S] cluster-containing enzymes, in the Δ*grxD* mutant and PAO1. Both strains showed no significant differences in the total activities of succinate dehydrogenase (9.4 $\pm$ 2.7 U/mg protein for the Δ*grxD* mutant, and 9.5 $\pm$ 0.9 U/mg protein for PAO1, respectively) and aconitase (33.9 $\pm$ 8.0 mU/mg protein for the Δ*grxD* mutant, and 35.9 $\pm$ 4.4 mU/mg protein for PAO1, respectively). The investigation was extended to test the effect of *grxD* inactivation on the regulatory functions of IscR and SoxR, which are [2Fe-2S] cluster containing transcriptional regulators. If GrxD is involved in either delivery of [2Fe-2S] clusters to or maturation of these proteins, we would anticipate alterations in the expression level and pattern of genes regulated by either IscR (*nfuA*, *tpx*, *fprB*, *iscA*, and *erpA*) or SoxR (*PA2274*) in the Δ*grxD* mutant. Quantitative reverse transcription (qRT)-PCR was performed using gene-specific primers (Table 1),

TABLE 1 Primers used in this study

Name	Sequence 5′→3′	Purpose
BT2781	GCCCGCACAAGCGGTGGAG	Forward primer for *16S rRNA*
BT2782	ACGTCATCCCCACCTTCCT	Reverse primer for *16S rRNA*
BT3367	CTGTTGAGGTAAGCCATGG	Forward primer for *grxD* coding region
BT3368	TCTTCGTCGGATGCGCGG	Reverse primer for *grxD* coding region
BT2871	ACAAGAGGATAATGGGCG	Forward primer for *erpA* coding region
BT2872	GCGGCGTTTTCGTAGCGG	Reverse primer for *erpA* coding region
BT2879	AACCGCTACGAGAACCTC	Forward primer for *nfuA* coding region
BT2880	TCGCCTCTTCTGCCTTAC	Reverse primer for *nfuA* coding region
EBI261	GCCATCAGCATGACCGAAGC	Forward primer for *iscA* coding region
EBI262	TCGCGAGTGAAGTCCAGCTC	Reverse primer for *iscA* coding region
BT2841	ACCATCCCGCAGCCCTG	Forward primer for *nfuA* expression
BT2860	ACCGCCATCGCCCTGAAG	Reverse primer for *nfuA* expression
BT2647	GAAGGATCAACGCAATGG	Forward primer for *tpx* expression
BT2649	ACCACGGTGTTGGCCAGC	Reverse primer for *tpx* expression
BT3551	GTCAACCGCAAGCGCTGATCG	Forward primer for *fprB* expression
BT3552	AGTCAGAGGCTGCACGTCGA	Reverse primer for *fprB* expression
BT3046	CCAGCGGGTCGGCATTCC	Forward primer for *soxR* expression
BT3047	AGGCCTGGAGCGACAGGC	Reverse primer for *soxR* expression
BT3351	ACCCGCCAGCCAGTTGTC	Forward primer for *PA2274* expression
BT3352	CACGCTTTTCGCCCCCAG	Reverse primer for *PA2274* expression
BT3612	GAAGATTTCGCCGGAGTCAA	Forward primer for *iscR* expression
BT3613	GCGTTCGGAGATATCGGCCAG	Reverse primer for *iscR* expression
BT7412	TGTTGAGGTCTCCAATGGACATCATCGAAACCATT	Forward primer for *grxD*-Strep tag protein expression
BT7413	CGTCGGGGTCTCGGCGCTGGCGTTGGCTTTGG	Reverse primer for *grxD*-Strep tag protein expression
BT7444	GACAGGGGTCTCTAATGCAAACCATCAAGGCTCTC	Forward primer for *ohr*-Strep tag protein expression
BT7445	GGAGAGGGTCTCGGCGCTGACCGACACGTTCAG	Reverse primer for *ohr*-Strep tag protein expression
BT7994	ACTCCCATGGAAACCATCAAGGCTC	Forward primer for *ohr*-His tag protein expression
BT8023	GAAGCTCGAGGACCGACACGTTCAG	Reverse primer for *ohr*-His tag protein expression

and total RNA was extracted from bacterial cultures grown under nonstressed and 0.5 mM plumbagin (PB)-treated (an inducer for SoxR [36, 37]) conditions. In the Δ*grxD* mutant, the expression levels and patterns of *soxR* and its target gene, *PA2274*, were not significantly different from that in PAO1 under uninduced or PB-induced conditions (Fig. 5A and B). In contrast, in the Δ*grxD* mutant under uninduced conditions, significant increases in the expression levels of *iscR* (2.4-fold), *nfuA* (2.1-fold), *tpx* (2.1-fold), *fprB* (2.8-fold), *iscA* (2.3-fold), and *erpA* (1.8-fold) were observed relative to that in PAO1. The increase in basal expression levels of these genes in the Δ*grxD* mutant was restored to PAO1 levels in the complemented mutant strain (Fig. 5A). However, deletion of *grxD* did not affect PB-induced expression of *iscR*, *nfuA*, *tpx*, and *fprB* (Fig. 5B). Furthermore, Western blot analysis was performed to observe the level of IscR. The results showed a 2.6-fold increase in the IscR level in the Δ*grxD* mutant under nonstressed conditions relative to that of wild-type PAO1 (Fig. 5C).

***P. aeruginosa* GrxD is involved in delivery of [Fe-S] clusters.** The [Fe-S] cluster delivery systems in *P. aeruginosa* have yet to be identified. In *E. coli*, ErpA and NfuA can function alone or ErpA can form a complex with NfuA giving rise to an oxidation-resistant [Fe-S] cluster delivery system. Because ErpA can complement some NfuA phenotypes (38), it seemed possible that iron-sulfur assembly components of other systems might compensate for the loss of GrxD. In order to determine the involvement of *P. aeruginosa* GrxD in either [Fe-S] cluster delivery or maturation, the expression plasmids pNfuA (39), pIscA (40), and pErpA (38) were introduced into the Δ*grxD* mutant strain, and their abilities to complement tBH-, CHP-, Dipy-, and PQ-sensitive phenotypes of the Δ*grxD* mutant were determined by plate sensitivity assay. The results in Fig. 6 show that the Δ*grxD* mutant was more sensitive to 1.0 mM tBH (40-fold), 1.8 mM CHP (10^2-fold), 1.2 mM Dipy (14-fold), and 0.15 mM PQ (10^2-fold) than PAO1. Expression of either *grxD*, *nfuA*, *iscA*, or *erpA* fully complemented the PQ-sensitive phenotype of the Δ*grxD* mutant to the wild-type level. The results illustrated that the [Fe-S] cluster

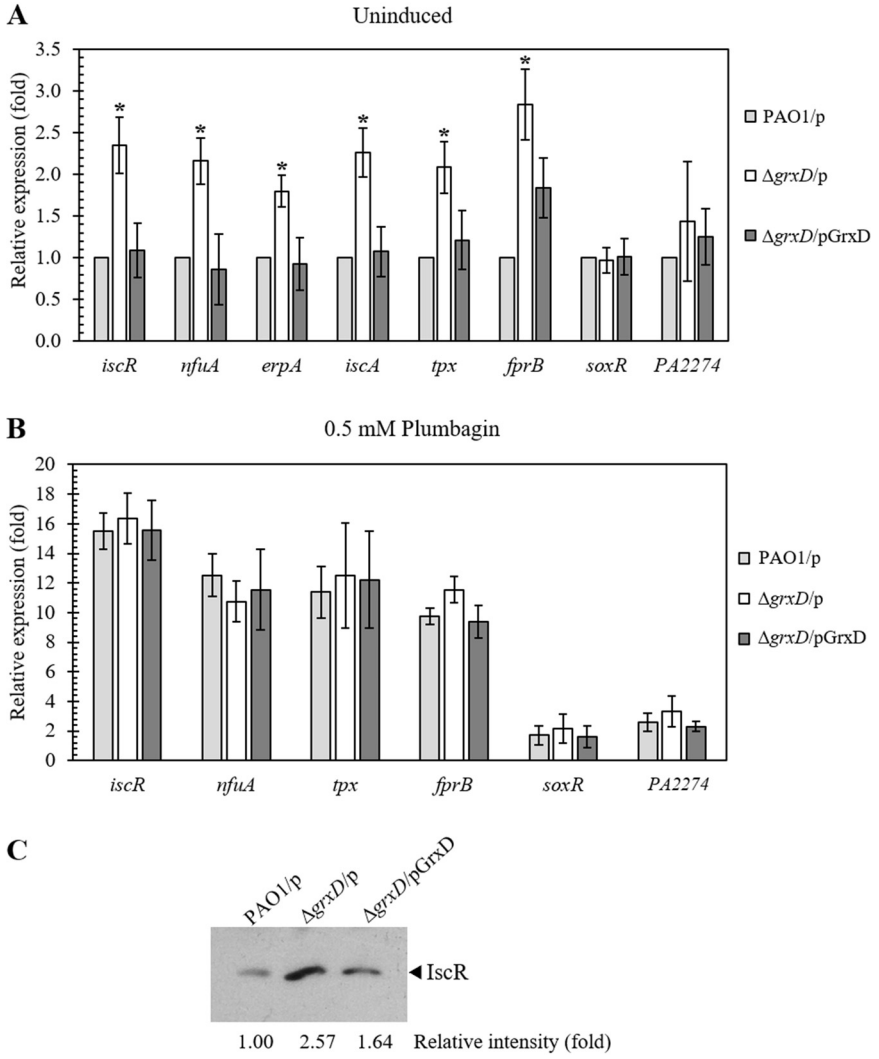

FIG 5 Expression levels of a [2Fe-2S] cluster containing transcriptional regulator and its target genes in the Δ*grxD* mutant. (A) Expression levels of *iscR* and its target genes were determined using reverse transcription (RT)-PCR. The RNA of exponential-phase cells of wild-type PAO1/p, Δ*grxD*/p, and Δ*grxD*/pGrxD was extracted. Relative expression was analyzed using the *16S rRNA* gene, and the result was expressed as the fold expression relative to the level of wild-type PAO1/p. (B) RT-PCR analysis of *iscR* and its target genes was performed under 0.5 mM plumbagin induction. (C) Western blot analysis of IscR protein in *grxD* mutant. Crude extracts were prepared from PAO1/p, Δ*grxD*/p, and Δ*grxD*/pGrxD cultures. Electrophoresis was carried out using 20 μg protein and 12.5% SDS-PAGE. The data shown are the means ± SD of three independent experiments. Asterisks indicate statistically significant differences ($P < 0.05$) relative to PAO1/p under uninduced conditions.

delivery proteins (NfuA, IscA, and ErpA) could functionally substitute for the lack of GrxD under PQ stress.

Moreover, ectopic expression of these [Fe-S] cluster delivery proteins from pNfuA, pIscA, and pErpA failed to restore the CHP-sensitive phenotype of the Δ*grxD* mutant to a wild-type level (Fig. 6). These results suggested that the role of GrxD in organic hydroperoxide protection is independent of GrxD's role in [Fe-S] cluster biosynthesis and trafficking.

Lack of GrxD attenuates virulence of *P. aeruginosa* in a *Drosophila* host model. In the pathogenic fungus *Cryptococcus neoformans*, monothiol Grx4 is important for iron homeostasis and virulence (41). The impact of *grxD* deletion on the virulence of *P. aeruginosa* was assessed using the fruit fly, *D. melanogaster*, as a host model. As shown in Fig. 7, feeding the flies with PAO1 cultures resulted in fly survivals of 50.8 ± 2.3%

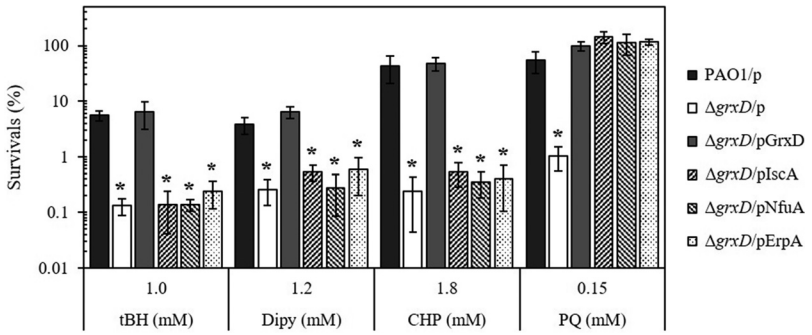

FIG 6 Determination of oxidant resistance levels in response to ectopic expression of genes encoding [Fe-S] cluster carrier proteins in a Δ*grxD* mutant background. Plate sensitivity assay results for PAO1/p, Δ*grxD*/p, Δ*grxD*/pGrxD, and Δ*grxD* mutant harboring a plasmid expressing [Fe-S] cluster carrier proteins, including *iscA* (Δ*grxD*/pIscA), *erpA* (Δ*grxD*/pErpA), and *nfuA* (Δ*grxD*/pNfuA) against 1.0 mM tBH, 1.2 mM Dipy, 1.8 mM CHP, and 0.15 mM PQ. The data shown are the means ± SD of three independent experiments.

(after incubation for 15 h) and 44.2 ± 1.8% (after incubation for 21 h) compared with 100 ± 0.0% (15 h) and 98.3 ± 0.5% (21 h) for LB medium as a control. Feeding the flies with the Δ*grxD* mutant resulted in a significant increase in fly survival (86.7 ± 1.0% and 81.7 ± 1.2% after incubation for 15 and 21 h, respectively) (Fig. 7). Hence, *grxD* deletion attenuated the virulence of PAO1 in the *D. melanogaster* model. The attenuated virulence phenotype was rescued in strain Δ*grxD*/pGrxD carrying a functional copy of *grxD* with fly survivals of 50.8 ± 1.7% and 41.7 ± 1.9% after incubation for 15 and 21 h, respectively.

DISCUSSION

The roles of monothiol Grxs in intracellular iron signaling, iron trafficking, and [Fe-S] cluster maturation protein have been reported in *C. neoformans* and *Aspergillus fumigatus* (41, 42). We have shown that the lack of *grxD* enhances the susceptibility to polymyxin antibiotics under both aerobic and anaerobic conditions (24). In this study, the Δ*grxD* mutant showed defects compared to PAO1, and impaired growth phenotypes have been observed in a *C. neoformans grx4* mutant (41). These phenotypes imply that the Δ*grxD* mutant has defects in coping with aerobic growth and/or oxidative stresses. The finding that the Δ*grxD* mutant had decreased resistance to superoxide and organic hydroperoxide stresses supported this assumption. These defects partially contribute to the growth-defect phenotype.

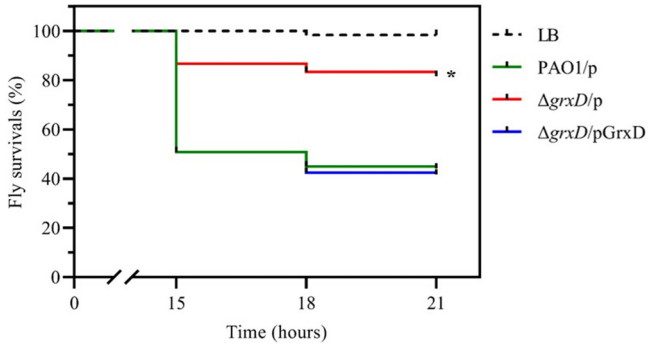

FIG 7 Survival curve of the fruit fly *D. melanogaster* infected with *P. aeruginosa* strains, measuring fly survival after feeding with PAO1/p, Δ*grxD*/p, and Δ*grxD*/pGrxD. Negative-control groups were treated with fresh LB medium. The experiments were independently repeated six times, and the pooled data were used to build the survival curves (n = 120). The percentage of fly survival was scored at indicated time points of infection after coincubation. The data presented are the means ± SD of three independent experiments. Asterisks indicate statistical significance ($P < 0.01$) determined using a log-rank (Mantel-Cox) test relative to PAO1/p.

Several studies have implicated Grxs in oxidative stress responses. A study in yeast has shown that the overexpression of *Grx1* or *Grx2* increased resistance to peroxides, including H_2O_2, tBH, and CHP. Furthermore, a strain lacking *Grx1* showed decreased resistance to tBH (43). However, a direct role of GrxD in protection of bacterial cells against oxidative stress has not been elucidated. We showed here that a Δ*grxD* mutant was highly sensitive to the superoxide-generating agent PQ, and organic hydroperoxides (CHP and tBH) (Fig. 3B). Moreover, the fact that the mutant phenotypes were also observed under anaerobic conditions, albeit at lower levels than under aerobic conditions, indicates an additional defect, which could arise from [Fe-S] delivery or maturation defects in important transcription regulators, such as IscR, Anr, and/or important anaerobic [Fe-S]-containing enzymes (37, 44). The impaired function of these transcription regulators may also be involved in the smaller colony and cell size observed in Δ*grxD* mutant grown under both aerobic and anaerobic atmospheres, relative to PAO1 wild type (Fig. 1B and 2A and B).

In many bacteria, the product of the organic hydroperoxide resistance gene *ohr* plays a primary role in organic hydroperoxide detoxification and protecting bacteria from organic hydroperoxide toxicity (30, 45, 46). Here, genetic and phenotypic analysis suggests that Ohr and GrxD function in the same pathway. The *in vitro* Ohr activity assays revealed remarkable results in that the use of a dithiol reductant, DTT, in combination with GrxD enhanced the efficiency of CHP degradation by Ohr over that of DTT alone (Fig. 4C and D). The *in vitro* protein-protein interaction experiments exhibit the direct binding between Ohr and GrxD (Fig. 4E). Thus, GrxD could act as the sole reductant in Ohr-mediated reduction of CHP *in vitro*, even though most monothiols lack the ability to support Ohr-mediated peroxidase activity (34, 35). In addition to conserved C29 of CGFS monothiol active site motif, GrxD contains an additional cysteine residue C42, which is thought to support GrxD's role as an alternative electron donor in the Ohr reaction. Nonetheless, cysteine mutational analysis of GrxD revealed that C29 at the active site is essential, while C42 did not participate in the ability of *grxD* to complement the organic hydroperoxide sensitivity of the Δ*grxD* mutant (Fig. 3B). The precise mechanism responsible for the significant increase in Ohr activity in the presence of dithiol and GrxD is not known. The question remains as to whether the enhancement of Ohr activity by GrxD *in vitro* is physiologically relevant, given that the enzyme uses thioredoxin and other thiols as reductants in the presence of GrxD (16, 47). The results from mutational and stress resistance analysis indicate that *grxD* physiologically contributes to the overall protection against organic hydroperoxide stress as shown by the significant reduction observed in the resistance level to CHP in the Δ*grxD* mutant (Fig. 3A and B). It remains to be seen whether this novel role for GrxD, i.e., as a reductant of Ohr, exists for other redox enzymes in *P. aeruginosa*.

The effect of GrxD inactivation on PQ sensitivity in the presence of O_2 suggested a link with [Fe-S] cluster biogenesis. This is supported by the finding that ectopic expression of [Fe-S] cluster biosynthesis and trafficking genes, including *erpA*, *iscA* and *nfuA*, can complement the PQ-sensitive phenotype of the Δ*grxD* mutant (Fig. 6). PQ is a superoxide generator/redox-cycling drug, capable of generating superoxide anion in the presence of oxygen (26, 48). Given that [Fe-S] clusters are a primary target for superoxide anions (11), we extended the investigation to probe for any functional links between GrxD and [Fe-S] containing proteins. This was indeed the case. In the Δ*grxD* mutant, we detected a defect in the function of the [2Fe-2S]-containing transcription regulator, IscR, which is an important global regulator of genes involved in [Fe-S] cluster biogenesis, resistance against oxidants, and pathogenicity (36, 37). In PAO1, IscR senses the cellular [Fe-S] cluster status and regulates the expression of genes involved in [Fe-S] biosynthesis (*iscRSUA-hscBA-fdx2-iscX*), *nfuA* (encodes [Fe-S] delivery protein), *tpx* (encodes thiol peroxidase), and *fprB* (encodes ferredoxin NADP [+] reductase) (22, 37, 39). IscR exists in two major forms: apo-IscR, which lacks a [2Fe-2S] center, and holo-IscR, which contains a [2Fe-2S]-IscR center. The two forms function as the transcriptional activator and repressor, respectively (21, 22, 36, 49). In *P. aeruginosa* under unstressed and iron-replete conditions, holo-IscR represses the expression of

the *isc* operon, which encodes proteins involved in [Fe-S] cluster biogenesis (21, 36). During iron starvation, or under conditions that damage [Fe-S] clusters, such as oxidative stress, IscR exists in the apo form. This results in derepression of the *isc* operon and apo-IscR-mediated activation of *fprB* expression to promote [Fe-S] cluster biogenesis (22).

Increases in the uninduced transcript levels of the apo-IscR activated gene, *fprB* (2.8-fold), and holo-IscR repressed genes *nfuA* (2.0-fold), *erpA* (1.8-fold), *iscA* (2.3-fold), and *tpx* (2.1-fold) confirm that holo-IscR function is compromised in the Δ*grxD* mutant. A relatively small increase in the basal transcript levels compared to the fully induced levels of these genes indicated that only a minor portion of IscR was in the apo-form, indicating that cells were defective in the transfer of newly formed [Fe-S] clusters to recipient proteins. However, no changes in the basal expression levels of *soxR* and its regulated gene *PA2274* were observed in the Δ*grxD* mutant. Unlike IscR, apo-SoxR is able to bind and repress transcription of its regulated promoters (50). Therefore, unchanged expression levels of *soxR* and *PA2274* could not reflect the [2Fe-2S] status of SoxR. Thus, the data indicate that GrxD is involved in facilitating [Fe-S] cluster delivery to and/or maturation of IscR. Furthermore, the Δ*grxD* mutant showed increased sensitivity to an intracellular iron-chelating agent (Dipy), indicating a decreased availability of free intracellular iron. In the *nfuA* mutant, for example, defects in [Fe-S] cluster maturation could lead to a decrease in the intracellular Fe^{2+} pool, resulting in increased sensitivity to the iron chelator, Dipy (39, 51).

The role of GrxD in repairing damaged [Fe-S] clusters has been demonstrated, in which a cysteine residue of GrxD couples with two GSH molecules for the ligation of the [2Fe-2S] cluster in Grx homodimer (10). *P. aeruginosa* GrxD contains a conserved CGFS motif within a monothiol Grx domain that contains a conserved cysteine residue, C29, and another nonconserved cysteine residue, C42. The C29, but not the nonconserved C42, is essential for GrxD function in PAO1 against PQ- and CHP-induced oxidative stresses. In *E. coli* Grx4, the C30 residue is equivalent to the C29 *P. aeruginosa* GrxD; each monomer of the dimer contributes to the coordination of the [Fe-S] cluster (52). This is consistent with our results, in which *P. aeruginosa* GrxD uses C29 as a principal cysteine residue for [Fe-S] cluster ligation to repair damaged [Fe-S] cluster containing proteins. In *E. coli*, monothiol GrxD is known to interact with BolA-like proteins forming [Fe-S]-bridge heterodimeric complexes to facilitate [2Fe-2S] cluster assembly and trafficking (17). An orthologous BolA-like protein has been predicted in *P. aeruginosa* (PA0857). Therefore, further studies are needed to examine the role of this protein.

The virulence testing using a *D. melanogaster* fly model revealed an attenuated killing phenotype of the Δ*grxD* mutant, indicating that GrxD contributes to the virulence of *P. aeruginosa* PAO1. In animals, one of the key components of the host innate immune response is the generation of superoxide anions ($O_2^{\cdot -}$) inside the phagolysosomes of the phagocytic cells (53). O_2^- is considered a starting point for the generation of more damaging ROS within the phagosome such as H_2O_2, hydroxyl radical, and peroxynitrite (54). Defects in the detoxification of $O_2^{\cdot -}$ are frequently associated with attenuated virulence (55, 56). This is true for *P. aeruginosa* PAO1, in which inactivation of genes encoding superoxide dismutase reduced bacterial virulence (57). Therefore, we speculate that attenuated virulence in the Δ*grxD* mutant is likely due to increased apo-IscR levels resulting from a defect in [Fe-S] cluster delivery and/or maturation in a selected group of [Fe-S] proteins. [Fe-S] clusters are prone to be oxidized by superoxide anions, as well as the redox-cycling drugs (58), thereby inactivating genes involved in [Fe-S] cluster biogenesis, and maturation, which also significantly attenuates virulence in *P. aeruginosa* (22, 39). In addition, the Δ*grxD* mutant showed increased sensitivity to organic hydroperoxide due to lowered Ohr activity resulting from the loss of GrxD as an electron donor. Although Ohr is associated with bacterial virulence in some microorganisms (59, 60), this is not the case for *P. aeruginosa*, in which an *ohr* mutant shows no virulence defect in the *D. melanogaster* model (61).

MATERIALS AND METHODS

Bacterial strains and growth conditions. All bacterial strains and plasmids used in this study are listed in Table 2. *P. aeruginosa* PAO1 and *E. coli* strains were aerobically cultivated in lysogeny broth (LB)

TABLE 2 Strains and plasmids used in this study

Strain or plasmid	Relevant characteristic (s)	Source
P. aeruginosa		
PAO1	Wild-type strain	ATCC 15692
PAO1/pBBR	PAO1 harboring pBBR1MCS-4	This study
Δ*grxD*	*grxD*-deleted mutant	24
Δ*grxD*/pBBR	Δ*grxD* mutant harboring pBBR1MSC-4, Cb^R	24
Δ*grxD*/pBBR-GrxD	Δ*grxD* mutant harboring pBBR-GrxD, Cb^R	24
Δ*grxD*/pBBR-GrxD-C29S	Δ*grxD* mutant harboring pBBR-GrxD-C29S, Cb^R	24
Δ*grxD*/pBBR-GrxD-C42S	Δ*grxD* mutant harboring pBBR-GrxD-C42S, Cb^R	24
Δ*grxD*/pBBR-GrxD-C29,C42S	Δ*grxD* mutant harboring pBBR-GrxD-C29,C42S, Cb^R	24
Δ*grxD*/pBBR-NfuA	Δ*grxD* mutant harboring pBBR-NfuA, Cb^R	This study
Δ*grxD*/pBBR-IscA	Δ*grxD* mutant harboring pBBR-IscA, Cb^R	This study
Δ*grxD*/pBBR-ErpA	Δ*grxD* mutant harboring pBBR-ErpA, Cb^R	This study
Plasmid		
pBBR-GrxD	pBBR1MCS-4 containing *grxD*	24
pBBR-GrxD-C29S	pBBR1MCS-4 containing *grxD*-C29S	24
pBBR-GrxD-C42S	pBBR1MCS-4 containing *grxD*-C42S	24
pBBR-GrxD-C29,C42S	pBBR1MCS-4 containing *grxD*-C29,C42S	24
pBBR-NfuA	pBBR1MCS-4 containing *nfuA*	This study
pBBR-IscA	pBBR1MCS-4 containing *iscA*	This study
pBBR-ErpA	pBBR1MCS-4 containing *erpA*	This study

at 37°C with shaking at 180 rpm. The medium for *E. coli* growth was supplemented with either 100 μg mL^{-1} ampicillin (Ap), 15 μg mL^{-1} gentamicin (Gm), 200 μg mL^{-1} carbenicillin (Cb), or 30 μg mL^{-1} Gm. Overnight cultures were inoculated into fresh LB medium; exponential growth phase cells (an optical density at 600 nm of 0.5, after 3 h of growth) were used in all experiments.

Molecular techniques. General molecular techniques, including DNA and RNA preparation, DNA cloning, PCR amplification, and *E. coli* transformation, were performed using standard protocols (62). Transformation of plasmids into *P. aeruginosa* strains was carried out using electroporation as previously described (63). The sequences of the oligonucleotide primers used are listed in Table 1.

Construction of [Fe-S] cluster delivery protein expression plasmids. The full-length of *erpA*, *iscA*, or *nfuA* containing the Shine-Dalgarno sequence was PCR amplified from PAO1 genomic DNA using primers BT2871 and BT2872 for *erpA*, EBI261 and EBI262 for *iscA*, or BT2879 and BT2880 for *nfuA* (Table 1). The PCR product was cloned into the medium-copy-number expression vector, pBBR1MCS-4, at the SmaI site to yield plasmids pErpA, pIscA, and pNfuA. The inserted genes were expressed from the *lac* promoter of the pBBR1MCS-4 vector.

qRT-PCR analysis. Quantitative real-time reverse transcription-PCR (qRT-PCR) was performed as previously described (37). Briefly, 10 ng of cDNA was added into a KAPA SYBR FAST qPCR kit as DNA templates for amplification with specific primers (Table 1) for 40 cycles of denaturation at 95°C for 20 s and extension at 60°C for 1 min. The *16S rRNA* amplified with primers BT2781 and BT2782 was used as a normalizing gene. The relative expression level, which was expressed as fold change relative to the level in wild-type PAO1 grown under uninduced conditions, was calculated using STEPONE software version 2.3. The difference in *Ct* values of each gene (ΔCt) between the *16S rRNA* and target gene levels is expressed as $\Delta Ct = Ct_{\text{target}} - Ct_{16s\ rRNA}$. The difference in ΔCt values ($\Delta\Delta Ct$) between tested sample and control sample was calculated. The expression ratio (fold change) was calculated from $2^{-\Delta\Delta Ct}$. The experiments were independently repeated three times, and the means ± standard deviations (SD) are shown.

Plate sensitivity assay. A plate sensitivity assays were performed to determine the oxidant resistance level as previously described (22). Briefly, exponential-phase cells were adjusted to optical density at 600 nm (OD_{600}) of 0.1 before making 10-fold serial dilutions. Then, 10 μL of each dilution was spotted onto LB agar plate containing appropriate concentrations of testing reagents. The plates were incubated overnight at 37°C before the CFU were scored. The percentage of survival was defined as the CFU on plates containing oxidant divided by the CFU on plates without oxidant and multiplied by 100.

GrxD and Ohr purification using Strep-tagged system. Strep-tagged GrxD and Ohr from *P. aeruginosa* were purified using the Strep tag for C-terminal fusion system as previously described (64). The coding regions of *grxD* and *ohr* were amplified from PAO1 genomic DNA with primers BT7412 and BT7413 for *grxD* and BT7444 and BT7445 for *ohr* coding regions, which contain BsaI site. The PCR products were digested with BsaI and cloned into BsaI-digested pASK-IBA3plus (IBA, Germany), generating the plasmid pStrep tag-GrxD and pStrep tag-Ohr, to produce Strep tag II fused to the C terminus of GrxD and Ohr. The Strep-tagged GrxD (13.0 kDa) and Strep-tagged Ohr (15.7 kDa) were overexpressed in *E. coli* DH5α and grown to an OD_{600} of 0.5 and then induced with 0.1 μg/mL anhydrotetracycline at 25°C overnight. Purification of the Strep-tagged GrxD and Strep-tagged Ohr was carried out using a Strep-Tactin Sepharose column as previously described (64).

***In vitro* pulldown assay.** The *in vitro* pulldown assay was performed using a Pierce ProFound pulldown polyHIS protein-protein interaction kit (Thermo Scientific) according to the manufacturer's

protocol. The interaction between purified Strep-tagged GrxD and 6×His-tagged Ohr was examined by incubating 100 μg of purified 6×His tag Ohr (Bait) with 50 μL of a 50% bed slurry of cobalt resin beads at 4°C for 1 h. Then, 400 μg of purified Strep tag GrxD (Prey) was added and incubated for 1 h at 4°C. After washing, bait-prey complexes were eluted using an elution buffer, separated on SDS-PAGE, and detected by Western blotting using the His tag and Strep tag antibodies.

Western blot analysis. Western blot analysis was performed as previously described (37). Briefly, bacterial cell lysates prepared from exponential-phase cultures were separated on12.5% SDS-PAGE and transferred to a Hybond polyvinylidene difluoride (PVDF) membrane (GE Healthcare Life Sciences). The blotted membrane was blocked with skimmed milk and hybridized with anti-His tag or anti-Strep tag antibody. Horseradish (HRP)-conjugated goat anti-rabbit antibodies (Invitrogen) were used as the secondary antibody. The membranes were developed using chemiluminescent HRP substrate (GE Healthcare, Germany) and Hyperfilm (GE Healthcare Life Sciences), and band intensity was measured using an ImageQuant LAS 4000 (GE Healthcare, Germany).

Ferrous ion oxidation xylenol orange (FOX) assay. The ability of bacteria to metabolize the cumene hydroperoxide (CHP) was determined using FOX assay as previously described (31). Briefly, the mid log-phase (OD_{600} = 0.5) of *P. aeruginosa* strains were treated with 100 μM CHP at 37°C. At various time points, the bacterial cultures were centrifuged at 12,000 rpm for 1 min to collect supernatant. The residual CHP in supernatant was determined by using the colorimetric method. A 100 μL of the supernatant was mixed with 900 μL of FOX reaction reagent (25 mM sulfuric acid, 0.2 mM ammonium ferrous sulfate, and 0.2 mM xylenol orange). After 10 min of incubation at room temperature, the residual hydroperoxide was measured at OD_{540}. The percentage of residual hydroperoxide was calculated by dividing OD_{540} of indicated time point with OD_{540} of control (derived by mixing oxidant with medium and immediately measuring the residual hydroperoxide) multiplying by 100. The data are presented as the means ± SD from three independent experiments.

Determination of *P. aeruginosa* cell length. Exponential-phase cells of *P. aeruginosa* strains were fixed on the glass slides and Gram stained before imaging through the light microscope (1,000×) connecting to the live mode imaging of a Nikon camera. The cell length was measured by microscope component tools in the Zeiss ZEN 2.3 Lite program under the same scale bar adjustment. The length of the six longest cells of five independent images in each strain (n = 30) were analyzed and expressed as the means ± SD.

***D. melanogaster* virulence tests.** The virulence of *P. aeruginosa* was evaluated using the *D. melanogaster* feeding assay as previously described (9, 65). Briefly, exponential-phase cultures of *P. aeruginosa* strains were adjusted to an OD_{600} of 0.5 before 800 μL of the bacterial cells were overlaid onto the surface of the preservative-free corn flour *Drosophila* medium at the bottom of glass fly culture vials. At 1 week old, adult flies were starved for 3 h prior to performing the feeding assay. Twenty flies were added to each vial, and each strain of *P. aeruginosa* was tested in at least three replicates. All of the tested flies were incubated at 25°C for 15 h before the number of viable flies was enumerated. The experiments were performed in a double-blind fashion and were analyzed from nine experiments using three different batches of flies.

Statistical and ethical statements. The significance of differences between strains or cultured conditions was statistically determined using Student's t test or Dunnett's *post hoc* test, with $P < 0.05$ considered a significant difference. All experiments handling *P. aeruginosa* and *D. melanogaster* were conducted following procedures MUSC2018-015 and MUSC61-056-458 and were approved by the Committee of Biosafety, Faculty of Science, Mahidol University (MUSC) and the MUSC Institutional Animal Care and Use Committee (IACUC), respectively.

ACKNOWLEDGMENTS

This work was supported by Thailand Science Research and Innovation, Chulabhorn Research Institute grant 2536703/42326 (http://www.cri.or.th/en/index.php). A.R. was financially supported by the Office of the Permanent Secretary, Ministry of Higher Education, Science, Research and Innovation through Research Grant for New Scholar RGNS63-183. The funders had no role in study design, data collection and interpretation, or the decision to submit the work for publication.

S.M. conceived and designed the experiments. K.S., A.R., J.D.-n., L.W., and P.L. performed the experiments. K.S., A.R., P.V., and S.M. analyzed the data. A.R. and S.M. contributed reagents, materials, and analysis tools. K.S., A.R., P.V., J.M.D., and S.M. wrote the paper.

We declare no conflict of interest.

REFERENCES

1. Lister PD, Wolter DJ, Hanson ND. 2009. Antibacterial-resistant *Pseudomonas aeruginosa*: clinical impact and complex regulation of chromosomally encoded resistance mechanisms. Clin Microbiol Rev 22:582–610. https://doi.org/10.1128/CMR.00040-09.
2. Hilliam Y, Kaye S, Winstanley C. 2020. *Pseudomonas aeruginosa* and microbial keratitis. J Med Microbiol 69:3–13. https://doi.org/10.1099/jmm.0.001110.
3. Yildiz EH, Airiani S, Hammersmith KM, Rapuano CJ, Laibson PR, Virdi AS, Hongyok T, Cohen EJ. 2012. Trends in contact lens-related corneal ulcers

at a tertiary referral center. Cornea 31:1097–1102. https://doi.org/10.1097/ICO.0b013e318221cee0.
4. Hancock JT, Desikan R, Neill SJ. 2001. Role of reactive oxygen species in cell signalling pathways. Biochem Soc Trans 29:345–350. https://doi.org/10.1042/0300-5127:0290345.
5. Ray PD, Huang BW, Tsuji Y. 2012. Reactive oxygen species (ROS) homeostasis and redox regulation in cellular signaling. Cell Signal 24:981–990. https://doi.org/10.1016/j.cellsig.2012.01.008.
6. Saenkham P, Eiamphungporn W, Farrand SK, Vattanaviboon P, Mongkolsuk S. 2007. Multiple superoxide dismutases in *Agrobacterium tumefaciens*: functional analysis, gene regulation, and influence on tumorigenesis. J Bacteriol 189:8807–8817. https://doi.org/10.1128/JB.00960-07.
7. Mongkolsuk S, Helmann JD. 2002. Regulation of inducible peroxide stress responses. Mol Microbiol 45:9–15. https://doi.org/10.1046/j.1365-2958.2002.03015.x.
8. Wei Q, Minh PN, Dotsch A, Hildebrand F, Panmanee W, Elfarash A, Schulz S, Plaisance S, Charlier D, Hassett D, Haussler S, Cornelis P. 2012. Global regulation of gene expression by OxyR in an important human opportunistic pathogen. Nucleic Acids Res 40:4320–4333. https://doi.org/10.1093/nar/gks017.
9. Wongsaroj L, Saninjuk K, Romsang A, Duang-Nkern J, Trinachartvanit W, Vattanaviboon P, Mongkolsuk S. 2018. *Pseudomonas aeruginosa* glutathione biosynthesis genes play multiple roles in stress protection, bacterial virulence and biofilm formation. PLoS One 13:e0205815. https://doi.org/10.1371/journal.pone.0205815.
10. Li H, Outten CE. 2012. Monothiol CGFS glutaredoxins and BolA-like proteins: [2Fe-2S] binding partners in iron homeostasis. Biochemistry 51:4377–4389. https://doi.org/10.1021/bi300393z.
11. Yeung N, Gold B, Liu NL, Prathapam R, Sterling HJ, Willams ER, Butland G. 2011. The *E. coli* monothiol glutaredoxin GrxD forms homodimeric and heterodimeric FeS cluster containing complexes. Biochemistry 50:8957–8969. https://doi.org/10.1021/bi2008883.
12. Herrero E, de la Torre-Ruiz MA. 2007. Monothiol glutaredoxins: a common domain for multiple functions. Cell Mol Life Sci 64:1518–1530. https://doi.org/10.1007/s00018-007-6554-8.
13. Stroher E, Millar AH. 2012. The biological roles of glutaredoxins. Biochem J 446:333–348. https://doi.org/10.1042/BJ20112131.
14. Rodriguez-Manzaneque MT, Ros J, Cabiscol E, Sorribas A, Herrero E. 1999. Grx5 glutaredoxin plays a central role in protection against protein oxidative damage in *Saccharomyces cerevisiae*. Mol Cell Biol 19:8180–8190. https://doi.org/10.1128/MCB.19.12.8180.
15. Rodriguez-Manzaneque MT, Tamarit J, Belli G, Ros J, Herrero E. 2002. Grx5 is a mitochondrial glutaredoxin required for the activity of iron/sulfur enzymes. Mol Biol Cell 13:1109–1121. https://doi.org/10.1091/mbc.01-10-0517.
16. Fernandes AP, Fladvad M, Berndt C, Andresen C, Lillig CH, Neubauer P, Sunnerhagen M, Holmgren A, Vlamis-Gardikas A. 2005. A novel monothiol glutaredoxin (Grx4) from *Escherichia coli* can serve as a substrate for thioredoxin reductase. J Biol Chem 280:24544–24552. https://doi.org/10.1074/jbc.M500678200.
17. Dlouhy AC, Li H, Albetel AN, Zhang B, Mapolelo DT, Randeniya S, Holland AA, Johnson MK, Outten CE. 2016. The *Escherichia coli* BolA protein IbaG forms a histidine-ligated [2Fe-2S]-bridged complex with Grx4. Biochemistry 55:6869–6879. https://doi.org/10.1021/acs.biochem.6b00812.
18. Santos JM, Lobo M, Matos AP, De Pedro MA, Arraiano CM. 2002. The gene *bolA* regulates *dacA* (PBP5), *dacC* (PBP6) and *ampC* (AmpC), promoting normal morphology in *Escherichia coli*. Mol Microbiol 45:1729–1740. https://doi.org/10.1046/j.1365-2958.2002.03131.x.
19. Boutigny S, Saini A, Baidoo EE, Yeung N, Keasling JD, Butland G. 2013. Physical and functional interactions of a monothiol glutaredoxin and an iron sulfur cluster carrier protein with the sulfur-donating radical *S*-adenosyl-L-methionine enzyme MiaB. J Biol Chem 288:14200–14211. https://doi.org/10.1074/jbc.M113.460360.
20. Giel JL, Rodionov D, Liu MZ, Blattner FR, Kiley PJ. 2006. IscR-dependent gene expression links iron-sulphur cluster assembly to the control of O_2-regulated genes in *Escherichia coli*. Mol Microbiol 60:1058–1075. https://doi.org/10.1111/j.1365-2958.2006.05160.x.
21. Giel JL, Nesbit AD, Mettert EL, Fleischhacker AS, Wanta BT, Kiley PJ. 2013. Regulation of iron-sulphur cluster homeostasis through transcriptional control of the Isc pathway by [2Fe-2S]-IscR in *Escherichia coli*. Mol Microbiol 87:478–492. https://doi.org/10.1111/mmi.12052.
22. Romsang A, Duang-Nkern J, Wirathorn W, Vattanaviboon P, Mongkolsuk S. 2015. *Pseudomonas aeruginosa* IscR-regulated ferredoxin $NADP^+$ reductase gene (*fprB*) functions in iron-sulfur cluster biogenesis and multiple stress response. PLoS One 10:e0134374. https://doi.org/10.1371/journal.pone.0134374.
23. Py B, Barras F. 2010. Building Fe-S proteins: bacterial strategies. Nat Rev Microbiol 8:436–446. https://doi.org/10.1038/nrmicro2356.
24. Romsang A, Leesukon P, Duangnkern J, Vattanaviboon P, Mongkolsuk S. 2015. Mutation of the gene encoding monothiol glutaredoxin (GrxD) in *Pseudomonas aeruginosa* increases its susceptibility to polymyxins. Int J Antimicrob Agents 45:314–318. https://doi.org/10.1016/j.ijantimicag.2014.10.024.
25. Winsor GL, Griffiths EJ, Lo R, Dhillon BK, Shay JA, Brinkman FS. 2016. Enhanced annotations and features for comparing thousands of *Pseudomonas* genomes in the *Pseudomonas* genome database. Nucleic Acids Res 44:D646–D653. https://doi.org/10.1093/nar/gkv1227.
26. Dietrich LE, Kiley PJ. 2011. A shared mechanism of SoxR activation by redox-cycling compounds. Mol Microbiol 79:1119–1122. https://doi.org/10.1111/j.1365-2958.2011.07552.x.
27. Boonma S, Romsang A, Duang-Nkern J, Atichartpongkul S, Trinachartvanit W, Vattanaviboon P, Mongkolsuk S. 2017. The FinR-regulated essential gene *fprA*, encoding ferredoxin NADP+ reductase: roles in superoxide-mediated stress protection and virulence of *Pseudomonas aeruginosa*. PLoS One 12:e0172071. https://doi.org/10.1371/journal.pone.0172071.
28. Zhang LB, Tang L, Ying SH, Feng MG. 2016. Regulative roles of glutathione reductase and four glutaredoxins in glutathione redox, antioxidant activity, and iron homeostasis of *Beauveria bassiana*. Appl Microbiol Biotechnol 100:5907–5917. https://doi.org/10.1007/s00253-016-7420-0.
29. Hassett DJ, Schweizer HP, Ohman DE. 1995. *Pseudomonas aeruginosa sodA* and *sodB* mutants defective in manganese- and iron-cofactored superoxide dismutase activity demonstrate the importance of the iron-cofactored form in aerobic metabolism. J Bacteriol 177:6330–6337. https://doi.org/10.1128/jb.177.22.6330-6337.1995.
30. Mongkolsuk S, Praituan W, Loprasert S, Fuangthong M, Chamnongpol S. 1998. Identification and characterization of a new organic hydroperoxide resistance (*ohr*) gene with a novel pattern of oxidative stress regulation from *Xanthomonas campestris* pv. phaseoli. J Bacteriol 180:2636–2643. https://doi.org/10.1128/JB.180.10.2636-2643.1998.
31. Ochsner UA, Hassett DJ, Vasil ML. 2001. Genetic and physiological characterization of *ohr*, encoding a protein involved in organic hydroperoxide resistance in *Pseudomonas aeruginosa*. J Bacteriol 183:773–778. https://doi.org/10.1128/JB.183.2.773-778.2001.
32. Si MR, Wang JB, Xiao X, Guan JY, Zhang YL, Ding W, Chaudhry MT, Wang Y, Shen XH. 2015. Ohr protects *Corynebacterium glutamicum* against organic hydroperoxide induced oxidative stress. PLoS One 10:e0131634. https://doi.org/10.1371/journal.pone.0131634.
33. Atichartpongkul S, Vattanaviboon P, Wisitkamol R, Jaroensuk J, Mongkolsuk S, Fuangthong M. 2016. Regulation of organic hydroperoxide stress response by two OhrR homologs in *Pseudomonas aeruginosa*. PLoS One 11:e0161982. https://doi.org/10.1371/journal.pone.0161982.
34. Cussiol JR, Alves SV, de Oliveira MA, Netto LE. 2003. Organic hydroperoxide resistance gene encodes a thiol-dependent peroxidase. J Biol Chem 278:11570–11578. https://doi.org/10.1074/jbc.M300252200.
35. Meireles DA, Domingos RM, Gaiarsa JW, Ragnoni EG, Bannitz-Fernandes R, da Silva Neto JF, de Souza RF, Netto LES. 2017. Functional and evolutionary characterization of Ohr proteins in eukaryotes reveals many active homologs among pathogenic fungi. Redox Biol 12:600–609. https://doi.org/10.1016/j.redox.2017.03.026.
36. Saninjuk K, Romsang A, Duang-Nkern J, Vattanaviboon P, Mongkolsuk S. 2019. Transcriptional regulation of the *Pseudomonas aeruginosa* iron-sulfur cluster assembly pathway by binding of IscR to multiple sites. PLoS One 14:e0218385. https://doi.org/10.1371/journal.pone.0218385.
37. Romsang A, Duang-Nkern J, Leesukon P, Saninjuk K, Vattanaviboon P, Mongkolsuk S. 2014. The iron-sulphur cluster biosynthesis regulator IscR contributes to iron homeostasis and resistance to oxidants in *Pseudomonas aeruginosa*. PLoS One 9:e86763. https://doi.org/10.1371/journal.pone.0086763.
38. Py B, Gerez C, Huguenot A, Vidaud C, Fontecave M, de Choudens SO, Barras F. 2018. The ErpA/NfuA complex builds an oxidation-resistant Fe-S cluster delivery pathway. J Biol Chem 293:7689–7702. https://doi.org/10.1074/jbc.RA118.002160.
39. Romsang A, Duang-Nkern J, Saninjuk K, Vattanaviboon P, Mongkolsuk S. 2018. *Pseudomonas aeruginosa nfuA*: gene regulation and its physiological roles in sustaining growth under stress and anaerobic conditions and maintaining bacterial virulence. PLoS One 13:e0202151. https://doi.org/10.1371/journal.pone.0202151.
40. Mapolelo DT, Zhang B, Naik SG, Huynh BH, Johnson MK. 2012. Spectroscopic and functional characterization of iron-bound forms of *Azotobacter*

vinelandii ^{Nif}IscA. Biochemistry 51:8056–8070. https://doi.org/10.1021/bi300664j.
41. Attarian R, Hu G, Sanchez-Leon E, Caza M, Croll D, Do E, Bach H, Missall T, Lodge J, Jung WH, Kronstad JW. 2018. The monothiol glutaredoxin Grx4 regulates iron homeostasis and virulence in *Cryptococcus neoformans*. mBio 9:e02377-18. https://doi.org/10.1128/mBio.02377-18.
42. Misslinger M, Scheven MT, Hortschansky P, Lopez-Berges MS, Heiss K, Beckmann N, Heigl T, Hermann M, Kruger T, Kniemeyer O, Brakhage AA, Haas H. 2019. The monothiol glutaredoxin GrxD is essential for sensing iron starvation in *Aspergillus fumigatus*. PLoS Genet 15:e1008379. https://doi.org/10.1371/journal.pgen.1008379.
43. Collinson EJ, Wheeler GL, Garrido EO, Avery AM, Avery SV, Grant CM. 2002. The yeast glutaredoxins are active as glutathione peroxidases. J Biol Chem 277:16712–16717. https://doi.org/10.1074/jbc.M111686200.
44. Trunk K, Benkert B, Quack N, Munch R, Scheer M, Garbe J, Jansch L, Trost M, Wehland J, Buer J, Jahn M, Schobert M, Jahn D. 2010. Anaerobic adaptation in *Pseudomonas aeruginosa*: definition of the Anr and Dnr regulons. Environ Microbiol 12:1719–1733. https://doi.org/10.1111/j.1462-2920.2010.02252.x.
45. Fontenelle C, Blanco C, Arrieta M, Dufour V, Trautwetter A. 2011. Resistance to organic hydroperoxides requires *ohr* and *ohrR* genes in *Sinorhizobium meliloti*. BMC Microbiol 11:100. https://doi.org/10.1186/1471-2180-11-100.
46. Si Y, Guo D, Deng S, Lu X, Zhu J, Rao B, Cao Y, Jiang G, Yu D, Zhong Z, Zhu J. 2020. Ohr and OhrR are critical for organic peroxide resistance and symbiosis in *Azorhizobium caulinodans* ORS571. Genes 11:335. https://doi.org/10.3390/genes11030335.
47. Hoffmann B, Uzarska MA, Berndt C, Godoy JR, Haunhorst P, Lillig CH, Lill R, Muhlenhoff U. 2011. The multidomain thioredoxin-monothiol glutaredoxins represent a distinct functional group. Antioxid Redox Signal 15:19–30. https://doi.org/10.1089/ars.2010.3811.
48. Hassan HM, Fridovich I. 1979. Paraquat and *Escherichia coli*: mechanism of production of extracellular superoxide radical. J Biol Chem 254:10846–10852. https://doi.org/10.1016/S0021-9258(19)86598-5.
49. Rajagopalan S, Teter SJ, Zwart PH, Brennan RG, Phillips KJ, Kiley PJ. 2013. Studies of IscR reveal a unique mechanism for metal-dependent regulation of DNA binding specificity. Nat Struct Mol Biol 20:740–747. https://doi.org/10.1038/nsmb.2568.
50. Hidalgo E, Bollinger JM, Jr, Bradley TM, Walsh CT, Demple B. 1995. Binuclear [2Fe-2S] clusters in the *Escherichia coli* SoxR protein and role of the metal centers in transcription. J Biol Chem 270:20908–20914. https://doi.org/10.1074/jbc.270.36.20908.
51. Angelini S, Gerez C, Ollagnier-de Choudens S, Sanakis Y, Fontecave M, Barras F, Py B. 2008. NfuA, a new factor required for maturing Fe/S proteins in *Escherichia coli* under oxidative stress and iron starvation conditions. J Biol Chem 283:14084–14091. https://doi.org/10.1074/jbc.M709405200.
52. Iwema T, Picciocchi A, Traore DA, Ferrer JL, Chauvat F, Jacquamet L. 2009. Structural basis for delivery of the intact [Fe2S2] cluster by monothiol glutaredoxin. Biochemistry 48:6041–6043. https://doi.org/10.1021/bi900440m.
53. Forman HJ, Torres M. 2001. Redox signaling in macrophages. Mol Aspects Med 22:189–216. https://doi.org/10.1016/s0098-2997(01)00010-3.
54. van Lith R, Ameer GA. 2016. Antioxidant polymers as biomaterial, p 251–296. *In* Dziubla T, Butterfield DA (ed), Oxidative stress and biomaterials. Academic Press, Boston, MA.
55. Liu NN, Uppuluri P, Broggi A, Besold A, Ryman K, Kambara H, Solis N, Lorenz V, Qi W, Acosta-Zaldivar M, Emami SN, Bao B, An D, Bonilla FA, Sola-Visner M, Filler SG, Luo HR, Engstrom Y, Ljungdahl PO, Culotta VC, Zanoni I, Lopez-Ribot JL, Kohler JR. 2018. Intersection of phosphate transport, oxidative stress and TOR signalling in *Candida albicans* virulence. PLoS Pathog 14:e1007076. https://doi.org/10.1371/journal.ppat.1007076.
56. Tsolis RM, Baumler AJ, Heffron F. 1995. Role of *Salmonella typhimurium* Mn-superoxide dismutase (SodA) in protection against early killing by J774 macrophages. Infect Immun 63:1739–1744. https://doi.org/10.1128/iai.63.5.1739-1744.1995.
57. Iiyama K, Chieda Y, Lee JM, Kusakabe T, Yasunaga-Aoki C, Shimizu S. 2007. Effect of superoxide dismutase gene inactivation on virulence of *Pseudomonas aeruginosa* PAO1 toward the silkworm, *Bombyx mori*. Appl Environ Microbiol 73:1569–1575. https://doi.org/10.1128/AEM.00981-06.
58. Mettert EL, Kiley PJ. 2015. How is Fe-S cluster formation regulated? Annu Rev Microbiol 69:505–526. https://doi.org/10.1146/annurev-micro-091014-104457.
59. Shea RJ, Mulks MH. 2002. *ohr*, encoding an organic hydroperoxide reductase, is an *in vivo*-induced gene in *Actinobacillus pleuropneumoniae*. Infect Immun 70:794–802. https://doi.org/10.1128/IAI.70.2.794-802.2002.
60. Reniere ML, Whiteley AT, Portnoy DA. 2016. An *in vivo* selection identifies *Listeria monocytogenes* genes required to sense the intracellular environment and activate virulence factor expression. PLoS Pathog 12:e1005741. https://doi.org/10.1371/journal.ppat.1005741.
61. Atichartpongkul S, Fuangthong M, Vattanaviboon P, Mongkolsuk S. 2010. Analyses of the regulatory mechanism and physiological roles of *Pseudomonas aeruginosa* OhrR, a transcription regulator and a sensor of organic hydroperoxides. J Bacteriol 192:2093–2101. https://doi.org/10.1128/JB.01510-09.
62. Sambrook J, Russell DW. 2001. Molecular cloning: a laboratory manual. Cold Spring Harbor Laboratory Press, Cold Spring Harbor, NY.
63. Choi KH, Kumar A, Schweizer HP. 2006. A 10-min method for preparation of highly electrocompetent *Pseudomonas aeruginosa* cells: application for DNA fragment transfer between chromosomes and plasmid transformation. J Microbiol Methods 64:391–397. https://doi.org/10.1016/j.mimet.2005.06.001.
64. Dokpikul T, Chaoprasid P, Saninjuk K, Sirirakphaisarn S, Johnrod J, Nookabkaew S, Sukchawalit R, Mongkolsuk S. 2016. Regulation of the cobalt/nickel efflux operon *dmeRF* in *Agrobacterium tumefaciens* and a link between the iron-sensing regulator rira and cobalt/nickel resistance. Appl Environ Microbiol 82:4732–4742. https://doi.org/10.1128/AEM.01262-16.
65. Romsang A, Duang-Nkern J, Khemsom K, Wongsaroj L, Saninjuk K, Fuangthong M, Vattanaviboon P, Mongkolsuk S. 2018. *Pseudomonas aeruginosa ttcA* encoding tRNA-thiolating protein requires an iron-sulfur cluster to participate in hydrogen peroxide-mediated stress protection and pathogenicity. Sci Rep 8:11882. https://doi.org/10.1038/s41598-018-30368-y.